Indian J. Pure Appl. Math., **51**(4): 1451-1469, December 2020
 DOI: 10.1007/s13226-020-0476-7

DISPERSION OF REACTIVE SPECIES IN CASSON FLUID FLOW

S. Debnath*, A. K. Saha**, B. S. Mazumder***[1] and A. K. Roy**

**Department of Mathematics, Indian Institute of Technology,*
Kharagpur 721 302, *India*
***Department of Mathematics, National Institute of Technology,*
Agartala 799 046, *India*
****Fluvial Mechanics Laboratory, Physics and Applied Mathematics Unit,*
Indian Statistical Institute, Kolkata 700 108, *India*
e-mail: sudipdebnath49@gmail.com

(*Received* 7 *January* 2019; *after final revision* 29 *June* 2019;
accepted 13 *September* 2019)

The study investigates the effect of wall reaction on the species transport in a pulsatile flow of Casson fluid through an annulus. The transport process is analyzed by means of the dispersion coefficient, which uses the technique of the method of moments. The equations of momentum along with the statistical moments are solved numerically using a finite difference implicit scheme. The distributions of mean and cross-sectional concentration are studied using the Hermite polynomial representation of central moments. The objective of this study is to focus on the nature of the dispersion coefficient due to the finite yield stress, amplitude of fluctuating pressure component, Womersley frequency parameter, radius ratio, and irreversible reaction rate. In contrast to previous other studies exist in the literature of solute dispersion in a non-Newtonian fluid, the present study discusses the cross-sectional concentration distribution of solute through an annulus. The study helps to enhance the understanding of all time behavior of dispersion phenomena under the proposed geometry, which may have applications to blood flow through the catheterized artery.

Key words : Dispersion coefficient; axial-mean concentration distribution; cross-sectional concentration distribution; Casson fluid; irreversible reaction.

2010 Mathematics Subject Classification : 76Z05, 92C10, 76A05, 35Q35, 65M06.

[1]Present address: Department of Civil Engineering, Indian Institute of Technology, Bombay 400 076, India

1. INTRODUCTION

Hydrodynamic dispersion describes the mass transport phenomena in processes which involve diffusion coupled with the flow, e.g., gas exchange in lungs, arterial blood flow, chromatography separation, flow through porous media, groundwater contamination, flow through microchannels, etc. Thus the study is of significant interest to many branches in science and engineering. Taylor [37] has initiated the study, which is the longitudinal evolution of the mean concentration over the cross-section and also known as Taylor dispersion, leading to a Gaussian distribution. Further, Aris [2] has introduced an alternative approach to investigate the dispersion phenomena using the concept of statistical moments. Basically, dispersion of solute refers to the stretching of a solute band in the flow direction during its transport by an advecting fluid which is often quantified in terms of the Taylor-Aris dispersion coefficient (Taylor [37] Aris [2]). Though the classical work of Taylor-Aris dispersion theory was only valid for a large time, several researchers contributed for further improvement of obtaining dispersion coefficient which is valid for all time. Gill and Sankarasubramanian [17] proposed a derivative expansion method known as 'generalized dispersion model', which held good for all instances. Further, Barton [5] refined Aris's method of moments and extended the legitimacy to cover even small and moderate times.

Due to its essential applications in polymer processing, biochemical processing, cardiovascular system, etc., the study of dispersion in the Newtonian and non-Newtonian fluid is always a matter of interest among the scientific community. The longitudinal dispersion of solute in steady or unsteady laminar flow in the presence (Sankarasubramanian and Gill [34], Mazumder and Das [20], Ng and Rudraiah [29], Paul and Mazumder [30], Rana and Murthy [31], Roy *et al*. [33]) or absence (Gill and Sankarasubramanian [18], Chatwin [8], Mukherjee and Mazumder [25], Dalal and Mazumder [9], Dash *et al*. [11], Nagarani and Sebastian [28]) of reaction at the boundary of pipe has been covered significantly over the years. Also, a few numbers of articles (Sarkar and Jayaraman [35], Mazumder and Paul [22], Roy *et al*. [32], Debnath *et al*. [12]) are found in literature who has considered the annular pipe flow for species transport in the longitudinal direction where some of them (Sarkar and Jayaraman [36], Mazumder and Mondal [21], Nagarani *et al*. [26, 27]) discuss the application of their model to the catheterized artery. In particular, the study of dispersion in Casson fluid has a lot of applications in physiological blood flow analysis; as the Casson fluid with respect to low yield stress is well appreciated (Charm and Kurland [7], Blair [6], McDonald [23]) to characterize blood flow analysis under the consideration of hematocrits, anticoagulants, temperature, etc.

Till now, Taylor dispersion is one of the most excellent methods to understand the axial transport of species through conduits. But it could be interesting if one investigates the cross-sectional concen-

tration distribution, which has not received much attention. Though the cross-sectional concentration distribution is vital related to environmental, industrial and biological applications, only a few numbers of articles can be found in literature who have considered the same for Newtonian fluid flow through pipe/channel. Using the homogenization technique, Wu and Chen [38] investigated the transverse uniformity of solute concentration distribution in a solvent flowing through a pipe. It has shown that the approach of the longitudinal normality of the mean concentration is faster than the approach to the transverse uniformity of the solute concentration. Wu *et al*. [39] studied the vertical distribution of contaminant in wetland flows, using the generalized dispersion technique of Gill [16]; further, the results are verified numerically. In a subsequent paper, Wu *et al*. [40] discussed the complete spatial concentration distribution pattern for laminar pipe flow. Fu *et al*. [15] studied the additional longitudinal displacement for contaminant dispersion in wetland flow by using Aris's concentration moments method. They also discussed the limitation of classical one-dimensional Taylor dispersion model for obtaining the additional displacement if the initial release of a contaminant is not uniform. In the presence of bed absorption in an open channel flow, Barik and Dalal [4] analyzed the transverse concentration distribution of species through a two-dimensional transport model. Combining analytical and numerical approaches, Wu and Singh [41] discussed the transport process in a laminar open channel flow under the effect of vertical position of a point-source solute release.

In the present study we have considered the followings: (a) flow through an annular pipe, (b) Casson fluid model as non-Newtonian nature of flowing stream, (c) flow oscillation due to the periodic pressure gradient, (d) heterogeneous first-order irreversible reaction at the outer wall of the annulus. The study represents the reliance of dispersion coefficient, axial mean concentration and cross-sectional concentration distributions with the functional parameters, viz., yield stress, radius ratio, irreversible absorption, etc. The significant part of this work is the cross-sectional concentration distribution of species in non-Newtonian Casson fluid, which has not considered previously.

2. MATHEMATICAL FORMULATION

Consider a fluid flow problem in an annular pipe having radius $\overline{a}$ (outer) and $\overline{b}$ (inner) ($\overline{a} > \overline{b}$) through which ($\overline{d} = \overline{a} - \overline{b}$, the region of stream and $\eta = \overline{b}/\overline{a}$, the fixed radius ratio) a Casson fluid is flowing axially under a periodic pressure gradient. The flow is assumed to be unsteady laminar, axisymmetric, incompressible and fully developed. The flow geometry is shown in Fig. 1, where $\overline{z}$ and $\overline{r}$ are the cylindrical coordinates in axial and radial direction. The pressure gradient at any $\overline{z}$ is given by

$$-\frac{\partial \overline{p}}{\partial \overline{z}} = A_0 + A_1 \sin(\omega_p \overline{t}), \tag{1}$$

where A_0 and A_1 are the amplitude of the steady and fluctuating component of pressure gradient, ω_p is the pulse frequency, $\overline{t}$ is time and $\overline{p}$ is pressure.

In the present situation the governing equation of motion can be written as:

$$\rho\frac{\partial\overline{u}}{\partial\overline{t}} = -\frac{\partial\overline{p}}{\partial\overline{z}} - \frac{1}{\overline{r}}\frac{\partial(\overline{r}\,\overline{\tau})}{\partial\overline{r}}, \tag{2}$$

where ρ, $\overline{u}(\overline{r},\overline{t})$ and $\overline{\tau}$ are the density, axial component of velocity and shear stress of the fluid respectively.

The non-linear relation between the shear stress and shear rate of Casson's constitutive equation (Aroesty and Gross [3]) is given by:

$$\left.\begin{array}{ll} \overline{\tau}^{\frac{1}{2}} = \overline{\tau}_y{}^{\frac{1}{2}} + (-\mu\,\frac{\partial\overline{u}}{\partial\overline{r}})^{\frac{1}{2}} & \text{if} \quad \overline{\tau} \geq \overline{\tau}_y, \\ \frac{\partial\overline{u}}{\partial\overline{r}} = 0 & \text{if} \quad \overline{\tau} \leq \overline{\tau}_y, \end{array}\right\} \tag{3}$$

here $\overline{\tau}_y$ and μ are the yield stress and viscosity of Casson fluid respectively. It can be interpreted from Eq. (3), if the shear stress exceeds the yield limit, a shear flow region is seen and the plug flow region can be observed when $\overline{\tau} \leq \overline{\tau}_y$.

Now we introduce a chemically active solute in the flowing fluid which is assumed to be so dilute that it will not materially affect in the carrier flow. The solute involves an irreversible absorption reaction at the outer wall of the annulus. We assume the concentration of the solute is $\overline{C}(\overline{t},\overline{r},\overline{z})$, which satisfies the transport equation,

$$\frac{\partial\overline{C}}{\partial\overline{t}} + \overline{u}(\overline{r},\overline{t})\frac{\partial\overline{C}}{\partial\overline{z}} = D\frac{\partial^2\overline{C}}{\partial\overline{z}^2} + \frac{D}{\overline{r}}\frac{\partial}{\partial\overline{r}}\left(\overline{r}\frac{\partial\overline{C}}{\partial\overline{r}}\right), \tag{4}$$

where D is the constant molecular diffusivity. The initial and boundary conditions for solving Eq. (4) are

$$\left.\begin{array}{l} \overline{C}(0,\overline{r},\overline{z}) = \overline{C}_0 B(\overline{r})\psi(\overline{z}), \quad (\overline{b} < \overline{r} < \overline{a}), \\ \psi(\overline{z}) = \overline{d}\;\delta(\overline{z}), \\ B(\overline{r}) = 1, \end{array}\right\} \tag{5}$$

$$\overline{C} = 0 \;\text{ as } \overline{z} \to \pm\infty \text{ for a finite extent of axial distribution,} \tag{6}$$

$$\frac{\partial\overline{C}}{\partial\overline{r}} = 0 \quad \text{at} \quad \overline{r} = \overline{b}, \tag{7}$$

$$\frac{\partial\overline{C}}{\partial\overline{r}} = -\overline{\Gamma}\,\overline{C} \quad \text{at} \quad \overline{r} = \overline{a}, \tag{8}$$

where $B(\overline{r})$ and $\psi(\overline{z})$ needed to be specified to solve Eq. (4), $\overline{C}_0$ is the initial concentration of slug input. We now introduce the following dimensionless quantities into Eqs. (1)-(8).

$$C = \frac{\overline{C}}{\overline{C}_0},\ u = \frac{\overline{u}}{U},\ U = -\frac{\overline{d}^2 A_0}{4\mu},\ r = \frac{\overline{r}}{\overline{d}},\ z = \frac{D\overline{z}}{\overline{d}^2\ U},\ t = \frac{D\overline{t}}{\overline{d}^2},\ \tau = \frac{\overline{\tau}}{\mu(\frac{U}{\overline{d}})},\ \tau_y = \frac{\overline{\tau}_y}{\mu(\frac{U}{\overline{d}})}. \tag{9}$$

Substituting Eq. (9) into Eqs. (4)-(8), we get

$$\frac{\partial C}{\partial t} + \ u(r,t)\frac{\partial C}{\partial z} = \frac{1}{r}\frac{\partial}{\partial r}\left(r\frac{\partial C}{\partial r}\right) + \frac{1}{Pe^2}\frac{\partial^2 C}{\partial z^2}, \tag{10}$$

$$C = 0 \ \text{ as } z \to \pm\infty, \tag{11}$$

$$\left.\begin{aligned} C(0,r,z) = B(r)\psi(z), \quad (r_{\rm i} < r < r_{\rm o}), \\ \psi(z) = \tfrac{\delta(z)}{Pe}, B(r) = 1, \end{aligned}\right\} \tag{12}$$

$$\frac{\partial C}{\partial r} = 0 \quad \text{at} \quad r = r_{\rm i}, \tag{13}$$

$$\frac{\partial C}{\partial r} = -\Gamma C \quad \text{at} \quad r = r_{\rm o}, \tag{14}$$

here $r_{\rm i}(=\ \eta/(1-\eta))$ and $r_{\rm o}(=\ 1/(1-\eta))$ are the dimensionless inner and outer radii of the annulus respectively. $Pe(=\ U\overline{d}/D)$ is the Péclet number, $\Gamma(=\ \overline{\Gamma}\ \overline{d})$ is the dimensionless irreversible absorption rate, represents the heterogeneous reaction at the outer wall of the annular tube.

3. Velocity Distribution

Utilizing the stress-strain relation (3) and the dimensionless quantities defined in Eq. (9) in the momentum Eq. (2) is re-written as:

$$\frac{1}{Sc}\frac{\partial u}{\partial t} = -4p(t) - \frac{\tau_y}{r} - \frac{2\sqrt{\tau}_y}{r}\left(-\frac{\partial u}{\partial r}\right)^{\frac{1}{2}} + \frac{1}{r}\frac{\partial u}{\partial r} + \frac{\partial^2 u}{\partial r^2}\left[1 + \sqrt{\tau}_y\left(-\frac{\partial u}{\partial r}\right)^{-\frac{1}{2}}\right], \tag{15}$$

here, $p(t) = 1 + e\ \sin(\alpha^2\ Sc\ t)$, $e = A_1/A_0$ and $\alpha^2 = \omega_p d^2/(\mu/\rho)$, where α is the Womersley frequency parameter and $Sc(=\ \nu/D)$ is the Schmidt number. The fluid velocity at the outer and inner wall of the annulus is supposed to be zero because of no-slip boundary conditions. The measure of plug core radius is estimated by the relation $r_p = \tau_y/p(t)$. The momentum Eq. (15) is a non-linear partial differential equation due to the Casson constitutive relation defined in Eq. (3), which is difficult to solve analytically. Thus to solve the momentum equation we have followed a finite difference Crank-Nicolson implicit scheme. The numerical method requires the velocity distribution at time $t = 0$. Here the steady velocity distribution is taken as an initial time velocity (similar to Nagarani *et al*. [26]). The detail of the proposed numerical technique is similar to Section 5. The

velocity distribution with the radius of pipe for various values of yield stress is shown in Fig. 2. It is seen that the velocity decreases as the value of yield stress increase, which completely agrees with Dash *et al.* [10].

4. METHOD OF MOMENTS

Following Aris [2], the p-th order concentration moment is defined as

$$C^{(p)}(t,r) \;=\; \int_{-\infty}^{+\infty} z^p C(t,r,z)dz. \tag{16}$$

Applying Eq. (16) to Eqs. (10)-(14), gives

$$\frac{\partial C^{(p)}}{\partial t} - \frac{1}{r}\frac{\partial}{\partial r}\left(r\frac{\partial C^{(p)}}{\partial r}\right) \;=\; p\,u(r,t)\,C^{(p-1)} + \frac{1}{Pe^2}p(p-1)C^{(p-2)}, \tag{17}$$

$$C^{(p)}(0,r) \;=\; \left\{ \begin{array}{ll} \frac{1}{Pe} & \text{for } p=0, \\ 0 & \text{for } p>0, \end{array} \right\} \tag{18}$$

$$\frac{\partial C^{(p)}}{\partial r} = 0 \quad \text{at} \quad r = r_i, \tag{19}$$

$$\frac{\partial C^{(p)}}{\partial r} = -\Gamma C^{(p)} \quad \text{at} \quad r = r_o. \tag{20}$$

The cross-sectional average of the p-th moment of the distribution of the solute is given by:

$$\left\langle C^{(p)}(t)\right\rangle = \frac{2}{r_o^2 - r_i^2}\int_{r_i}^{r_o} rC^{(p)}(t,r)dr, \tag{21}$$

where $\langle . \rangle$ denotes the cross-sectional mean.

Using Eq. (21) to Eq. (17) and Eq. (18), gives

$$\frac{\mathrm{d}}{\mathrm{d}t}\left\langle C^{(p)}\right\rangle + \frac{2r_o\Gamma}{r_o^2 - r_i^2}C^{(p)}(t,r_o) = \; p\left\langle u(r,t)C^{(p-1)}\right\rangle + \frac{1}{Pe^2}\,p(p-1)\left\langle C^{(p-2)}\right\rangle, \tag{22}$$

$$\left.\begin{array}{rll} \left\langle C^{(p)}(0)\right\rangle = & \dfrac{1}{Pe} & \text{for } p=0, \\ = & 0 & \text{for } p>0. \end{array}\right\} \tag{23}$$

The p-th order central moment about mean of the concentration distribution is defined as

$$\mu_p(t) = \frac{\int_{r_i}^{r_o}\int_0^{2\pi}\int_{-\infty}^{+\infty} r(z-z_g)^p C\mathrm{d}r\mathrm{d}\theta\mathrm{d}z}{\int_{r_i}^{r_o}\int_0^{2\pi}\int_{-\infty}^{+\infty} rC\mathrm{d}r\mathrm{d}\theta\mathrm{d}z}, \tag{24}$$

where

$$z_g = \frac{\int\int\int zC\mathrm{d}v}{\int\int\int C\mathrm{d}v} = \frac{\left\langle C^{(1)}\right\rangle}{\left\langle C^{(0)}\right\rangle},$$

is the longitudinal centroid of the solute concentration and $\left\langle C^{(0)}\right\rangle$ is the total mass of the chemical species in the bulk flow. For different values of p in Eq. (24), one can obtain expression of central moments, such as, $p = 2$, gives

$$\mu_2(t) = \frac{\left\langle C^{(2)}\right\rangle}{\left\langle C^{(0)}\right\rangle} - z_g^2. \tag{25}$$

Equation (25) is the second order central moment represents the variance of solute concentration. According to Aris [2], the rate of change of variance is proportional to the sum of the molecular diffusion coefficient along the axial direction and apparent dispersion coefficient in the radial direction. As the axial diffusion is minor in comparison with the lateral diffusion, the apparent dispersion coefficient D_c can be written as:

$$D_c = \frac{1}{2}\frac{d\mu_2}{dt}. \tag{26}$$

From the first two moments, the distribution can be analyzed sufficiently as it finally tends to normal. But to measure the degree of symmetry and peakedness of the concentration distribution, the role of third and fourth order central moments are also important as they are required to obtain the coefficients of Skewness ν_2 and Kurtosis ν_3 respectively. The expression of third and fourth order central moments can be obtained from Eq. (24) for $p = 3$ and 4, as

$$\left.\begin{aligned} \mu_3(t) &= \frac{\left\langle C^{(3)}\right\rangle}{\left\langle C^{(0)}\right\rangle} - 3z_g\mu_2 - z_g^3, \\ \mu_4(t) &= \frac{\left\langle C^{(4)}\right\rangle}{\left\langle C^{(0)}\right\rangle} - 4z_g\mu_3 - 6z_g^2\mu_2 - z_g^4. \end{aligned}\right\} \tag{27}$$

In the next section, the detail numerical scheme is discussed for the moment differential equation, the same has been followed for the numerical solution of momentum equation.

5. Numerical Solution

In order to solve Eq. (17) along with the initial and boundary conditions (18)-(20), we have adopted a finite difference method based on Crank Nicolson implicit scheme. With this motive, we divide the width of the annular gap into $(M-1)$ equal parts of length $\Delta r = (b-a)/(M-1)$ represented by the grid point j. Thus the grid point $j = 1$ address the inner wall $r = r_i$ and $j = M$ address the outer wall $r = r_o$, in general $r_j = r_i + (j-1) \times \Delta r$. Similarly, we have discretized the time by the grid

point i of length Δt by the relationship $t_i = (i-1) \times \Delta t$. So, $i = 1$ indicates the initial time $t = 0$. This discretization leads to a system of linear equation with a tridiagonal coefficient matrix:

$$P_j C^{(p)}(i+1, j+1) + Q_j C^{(p)}(i+1, j) + R_j C^{(p)}(i+1, j-1) = S_j, \tag{28}$$

where P_j, Q_j, R_j and S_j are the matrix elements. The finite difference form of the initial and boundary conditions are

$$C^{(p)}(1, j) \quad = \quad \left\{ \begin{array}{ll} \frac{1}{Pe} & \text{for } p = 0, \\ 0 & \text{for } p > 0, \end{array} \right\} \tag{29}$$

and

$$\begin{aligned} &C^{(p)}(i+1, 0) = C^{(p)}(i+1, 2), \text{ (at the surface of the inner cylinder);} \\ &C^{(p)}(i+1, M+1) = C^{(p)}(i+1, M-1) - 2\Gamma \Delta r C^{(p)}(i+1, M), \text{ (at the surface of the outer cylinder).} \end{aligned} \tag{30}$$

To solve this tridiagonal system a matlab code has developed implementing the Thomas algorithm (Anderson *et al.* [1]). The detail of the computational steps are mentioned as:

First, the axial velocity $u(r, t)$ is computed from Eq. (15) at all grid points. *Second*, as we have the solution of $u(r, t)$, the p-th order concentration moment $C^{(p)}(r, t)$ is evaluated from Eq. (17). *Third*, integrating $rC^{(p)}$ by Simpson's one-third rule, finally $\left\langle C^{(p)}(t) \right\rangle$ is calculated from Eq. (21).

Numerical computation is accomplished for steady and pulsatile characteristics of velocity distribution. For any finite value of $\Delta t/(\Delta r)^2$, the present scheme is linearly stable where a mesh size ($\Delta t = 0.00001$, $\Delta r = 1/(M-1)$) and $M = 100$ provide a decent results under the variation of parameters. During the study, we always consider the value of Pe and Sc is 1000. By altering the time step and grid spacing follows from the above spatial and temporal discretization parameters, an excellent order of accuracy of the results is assured. The dispersion process affected by the pulsatile nature of the stream can be well established when the time interval is small enough, while to manage the efficiency of the results, sufficiently smaller space discretization is required.

6. Distributions of Mean and Cross-sectional Concentration

The distribution of axial mean concentration can be observed using the first few central moments. There are lots of article (Mehta *et al.* [24], Debnath *et al.* [13, 14]) found in literature who has studied the axial distribution of mean concentration $C_m(t, z)$ using the Hermite polynomial representation of first four central moments. In the present study, we also consider the same approach to understand

the effect of various parameter on the axial mean concentration distribution, which gives

$$C_m(t,z) = \left\langle C^{(0)}(t) \right\rangle e^{-\chi^2} \sum_{n=0}^{\infty} A_n(t) H_n(\chi), \tag{31}$$

where $\chi = (z - z_g)/\sqrt{2\mu_2},\ z_g = \left\langle C^{(1)} \right\rangle / \left\langle C^{(0)} \right\rangle$ and H_i's are Hermite polynomials that satisfy the recurrence relation:

$$H_{i+1}(\chi) = 2\chi H_i(\chi) - 2iH_{i-1}(\chi), \quad i = 0, 1, 2, \ldots (H_0(\chi) = 1).$$

The coefficients A_i's are

$$A_0 = 1/\left(2\pi\mu_2\right)^{1/2}, \quad A_1 = A_2 = 0, \quad A_3 = 2^{1/2} A_0 \nu_2/24, \quad A_4 = A_0\nu_3/96.$$

Having the central moments from Eqs. (25) and (27), the required axial mean concentration distribution can be obtained from Eq. (31) at any given location and time.

It is worthwhile to note that the axial dispersion coefficient is proportional to the time derivative of μ_2, which has obtained by taking the cross-sectional average of p-th moment of the solute distribution defined in Eq. (21) and from the intermediate relationship between raw and central moments given in Eq. (25). Similarly, to evaluate the axial mean concentration, those first four central moments are required. But to explore more on the dispersion process, the cross-sectional concentration distribution of solute is significant, which is also new in this arena of research. To see the variation of cross-sectional concentration distribution one has to avoid the cross-sectional average of the p-th moment of the solute distribution. Then the resulting central moments should be a function of time t and radius r, though the expressions are analogous to Eqs. (25) and (27). Now using these central moments and with the help of Hermite polynomial, the cross-sectional concentration distribution can be approximated as discussed earlier. In a recent work of Li *et al*. [19] also investigates the spatial concentration distribution using the same technique for an open channel flow driven by gravity and wind. The general expression of concentration is similar like Eq. (31), instead of $C_m(t,z)$ it must be $C(t,r,z)$, the coefficients of A_i's and the Hermite polynomials H_is should be function of r and t respectively.

7. Results and Discussion

The study of dispersion in a Casson fluid flow through an annulus is of considerable interest because of its application in the analysis of the flow of blood through the catheterized artery. Aris-Barton method of moments is proposed to analyze the behavior of solute transport in terms of the dispersion

coefficient, which has estimated using a finite difference implicit scheme. Two different cases have been taken to verify the adopted numerical scheme, as:

Case I : In the presence of wall reaction, if $\eta \to 0$ and $\tau_y = 0$, the present model becomes a circular pipe model, a case studied by Mazumder and Das [20] under time-dependent Hagen-Poiseuille flow of Newtonian fluid. Fig. 3(a) shows the axial distribution of mean concentration at different instants of time due to the combined flow situation, qualitatively agrees with the result of Mazumder and Das [20].

Case II : The present model is analogous to the study of dispersion in Dash *et al*. [11] with the absence of boundary reaction (i.e., $\Gamma = 0$) when $\eta \to 0$. It has seen that the obtained result (Fig. 3(b)) is fully agreed with them.

Following subsections discuss the solute dispersion coefficient, axial mean concentration distribution, and cross-sectional concentration distribution due to various values of parameters. Two time intervals such as [0-0.08] and [0.42-0.5] are considered to see the small and large time behavior of dispersion coefficient.

7.1 *Axial dispersion coefficient*

In Fig. 4, the effect of irreversible reaction rate Γ on the dispersion coefficient D_c is shown for small (Fig. 4(a)) and large (Fig. 4(b)) interval of time. It is seen that as the value of Γ increases the value of D_c decrease for all-time, which is in agreement with the nature of irreversible absorptive reaction on the solute dispersion process. A similar kind of behavior of dispersion coefficient due to the heterogeneous irreversible reaction in pipe flow of Casson fluid has been observed and reasoned by Rana and Murthy [31].

The solute dispersion process largely depends on the fluid velocity, and we know for the case of a Casson fluid flow the yield stress played a major rule. Thus, to study the dispersion of a solute in a non-Newtonian Casson fluid, yield stress effect is an important case. Fig. 5 depicts the time variation of dispersion coefficient with respect to the yield stress for small and large time. It has seen that the value of the dispersion coefficient is increasing with time, though after a fixed time it reaches to a non-transient state. For all time, an increment in the value of yield stress always decreases the magnitude of the dispersion coefficient. As the fluid velocity reduces due to the increase of yield stress, axial dispersion coefficient found to decline.

In the present study, we consider an annular pipe as the flow geometry, which is motived to understand the indicator dilution technique in a catheterized artery. Here the outer pipe is assumed to

be the blood vessel and the inner pipe within it makes the formation of an annular region between the catheter wall and the arterial wall. For the purpose of measurement, this kind of catheters is mostly used to inject dye and withdraw blood samples. So the radius ratio of an annular pipe may control the diffusion process while transporting species through it. In Fig. 6 the time assessment of dispersion coefficient with the variation of radius ratio η is shown. The dispersion coefficient is found to decrease significantly with the radius ratio of the annulus which is due to the reduction of velocity with the increase of radius ratio.

The effect of amplitude of the fluctuating pressure component e on the dispersion coefficient D_c is shown in Fig. 7, where the larger values of e make an increment of D_c for all time. Initially, D_c is found to increase with time, but the oscillation become uniform after a fixed instant of time. Though the dispersion coefficient reduces with Womersley number α (Fig. 8). It has seen that for larger values of α, dispersion coefficient reaches early to a non-transient state.

7.2 *Mean concentration distribution*

The axial distribution of mean concentration $C_m(t, z)$ is shown in Fig. 9 due to the pulsatile nature of fluid velocity. Fig. 9(a) depicts the effect of irreversible reaction rate Γ on C_m at a fixed dimensionless time $t = 0.15$, whereas Fig. 9(b) shows the same at time $t = 0.5$ respectively. It is observed from the Figs. 9(a, b) that because of higher values of irreversible reaction rate at the boundary, the peak of the mean concentration always goes downward. Also at the large time, the distribution become much flat due to the strong absorption rate.

Variation of mean concentration $C_m(t, z)$ towards the axial distance is presented in Fig. 10 for different values of yield stress τ_y. As like the previous figure, here in Figs. 10(a, b), we also consider two fixed times. In both cases, the peak of the mean concentration distribution is found to increase as the value of yield stress increases. For all time, the dispersion coefficient is reduced by the yield stress and hence peak of the mean concentration distribution is increased.

7.3 *Cross-sectional concentration distribution*

In Figs. 11(a, b), the cross-sectional concentration distribution is shown due to different values of absorption rate Γ at fixed time $t = 0.5$ and 1. From both the figures it can be seen that the peak of the concentration distribution decreases as Γ increase. The reason is quite natural, because of the high absorption rate maximum number of moles of solute undergoing chemical reaction at the outer wall of the annulus. It must be noticed that there is a clear difference between the value of concentration at the inner and outer wall. The concentration at the outer wall is very less as compared to the inner wall, which may be the presence of reaction (absorption) at the outer wall. Almost all the different values

of Γ, the concentration difference is negligible at the inner wall. At the center of the flow region, the velocity is maximum for a laminar pipe flow; thus, a higher concentration zone is observed there.

The effect of yield stress τ_y on the cross-sectional concentration distribution of solute is analyzed through Figs. 12(a, b). Here we also compare the results for Newtonian ($\tau_y = 0$) and non-Newtonian Casson fluid ($\tau_y = 0.02, 0.04$) models. At a fixed time, the area under the distribution curve is higher for Casson fluid than the Newtonian fluid. As yield stress enhances the flow resistance, so it is obvious that the peak of the concentration distribution increase with the augmentation of yield stress (Fig. 12).

8. CONCLUSION

A numerical study on the dispersion of a reactive solute in a pulsatile flow of Casson fluid through an annular pipe is discussed in the present work. Apart from the dispersion coefficient, and mean concentration distribution the study also investigates the cross-sectional concentration distribution. The conclusions that can be made from the present investigation are as follows:

(a) The magnitude of the dispersion coefficient D_c is a decreasing function of irreversible reaction rate Γ, yield stress τ_y and radius ratio η, for all time.

(b) As the value of the amplitude of fluctuating pressure component e increases, dispersion coefficient D_c increase, whereas an opposite trend is captured for Womersley frequency parameter α.

(c) The peak of the mean concentration C_m profile goes down as the irreversible reaction rate Γ increase, though the same goes upward when the yield stress τ_y take larger values.

(d) The peak of the cross-sectional concentration distribution increases due to higher values of yield stress. An opposite scenario has been observed for the case of boundary reaction rate constant.

(e) The results obtained from the present study are satisfied well with those of the existing works, under limiting conditions.

ACKNOWLEDGEMENT

The authors are grateful to the editor and reviewers for the valuable comments and suggestions that helped to improve this article.

REFERENCES

1. D. Anderson, J. C. Tannehill, and R. H. Pletcher, *Computational Fluid Mechanics and Heat Transfer*, Hemisphere Publishing Corporation, New York (1984).
2. R. Aris, On the dispersion of a solute in a fluid flowing through a tube, *Proc. R. Soc. London, Ser. A*, **235** (1956), 67-77.
3. J. Aroesty and J. F. Gross, The mathematics of pulsatile flow in small blood vessels: I. Casson Theory, *Microvasc. Res.*, **4** (1972), 1-12.
4. S. Barik and D. C. Dalal, Transverse concentration distribution in an open channel flow with bed absorption: A multi-scale approach, *Commun. Nonlinear Sci. Numer. Simul.*, **65** (2018), 1-19.
5. N. G. Barton, On the method of moments for solute dispersion, *J. Fluid Mech.*, **126** (1983), 205-218.
6. G. W. S. Blair, An equation for the flow of blood, plasma and serum through glass capillaries, *Nature*, **183** (1959), 613-614.
7. S. Charm and G. Kurland, Viscometry of human blood for shear rates of 0-100,000 $\sec^{-1}$, *Nature*, **206** (1965), 617-618.
8. P. C. Chatwin, On the longitudinal dispersion of passive contaminant in oscillatory flows in tubes, *J. Fluid Mech.*, **71** (1975), 513-527.
9. D. C. Dalal and B. S. Mazumder, Unsteady convective diffusion in viscoelastic fluid flowing through a tube, *Int. J. Non Linear Mech.*, **33** (1998), 135-150.
10. R. K. Dash, G. Jayaraman, and K. N. Mehta, Estimation of increased flow resistance in a narrow catheterized arterya theoretical model, *J. Biomech.*, **29** (1996), 917-930.
11. R. K. Dash, G. Jayaraman, and K. N. Mehta, Shear augmented dispersion of a solute in a Casson fluid flowing in a conduit, *Ann. Biomed. Eng.*, **28** (2000), 373-385.
12. S. Debnath, S. Paul, and A. K. Roy, Transport of Reactive Species in Oscillatory Annular Flow, *J. Appl. Fluid Mech.*, **11** (2018), 405-417.
13. S. Debnath, A. K. Saha, B. S. Mazumder, and A. K. Roy, Dispersion phenomena of reactive solute in a pulsatile flow of three-layer liquids, *Phys. Fluids*, **29** (2017), 097107.
14. S. Debnath, A. K. Saha, B. S. Mazumder, and A. K. Roy, Hydrodynamic dispersion of reactive solute in a Hagen-Poiseuille flow of a layered liquid, *Chin. J. Chem. Eng.*, **25** (2017), 862-873.
15. X. Fu, R. Gao, and Z. Wu, Additional longitudinal displacement for contaminant dispersion in wetland flow, *J. Hydrol.*, **532** (2016), 37-45.
16. W. N. Gill, A note on the solution of transient dispersion problems, *Proc. R. Soc. London, Ser. A*, **298** (1967), 335-339.

17. W. N. Gill and R. Sankarasubramanian, Exact analysis of unsteady convective diffusion, *Proc. R. Soc. London, Ser. A*, **316** (1970), 341-350.

18. W. N. Gill and R. Sankarasubramanian, Dispersion of non-uniformly distributed time-variable continuous sources in time-dependent flow, *Proc. R. Soc. London, Ser. A*, **327** (1972), 191-208.

19. G. Li, W. Jiang, P. Wang, J. Guo, Z. Li, and G. Q. Chen, Concentration moments based analytical study on Taylor dispersion: Open channel flow driven by gravity and wind, *J. Hydrol.*, **562** (2018), 244-253.

20. B. S. Mazumder and S. K. Das, Effect of boundary reaction on solute dispersion in pulsatile flow through a tube, *J. Fluid Mech.*, **239** (1992), 523-549.

21. B. S. Mazumder and K. K. Mondal, On solute transport in oscillatory flow through an annular pipe with a reactive wall and its application to a catheterized artery, *Quart. J. Mech. Appl. Math.*, **58** (2005), 349-365.

22. B. S. Mazumder and S. Paul, Dispersion of reactive species with reversible and irreversible wall reactions, *Heat Mass Transfer*, **48** (2012), 933-944.

23. D. A. McDonald, *Blood flow in arteries*, Edward Arnold, London (1974).

24. R. V. Mehta, R. L. Merson, and B. J. McCoy, Hermite polynomial representation of chromatography elution curves, *J. Chromatogr. A*, **88** (1974), 1-6.

25. A. Mukherjee and B. S. Mazumder, Dispersion of contaminant in oscillatory flows, *Acta Mech.*, **74** (1988), 107-122.

26. P. Nagarani, G. Sarojamma, and G. Jayaraman, Exact analysis of unsteady convective diffusion in Casson fluid flow in an annulus–Application to catheterized artery, *Acta Mech.*, **187** (2006), 189-202.

27. P. Nagarani, G. Sarojamma, and G. Jayaraman, Effect of boundary absorption on dispersion in Casson fluid flow in an annulus: application to catheterized artery, *Acta Mech.*, **202** (2009), 47-63.

28. P. Nagarani and B. T. Sebastian, Dispersion of a solute in pulsatile non-Newtonian fluid flow through a tube, *Acta Mech.*, **224** (2013), 571-585.

29. C. O. Ng and N. Rudraiah, Convective diffusion in steady flow through a tube with a retentive and absorptive wall, *Phys. Fluids*, **20** (2008), 073604.

30. S. Paul and B. S. Mazumder, Effects of nonlinear chemical reactions on the transport coefficients associated with steady and oscillatory flows through a tube, *Int. J. Heat Mass Transfer*, **54** (2011), 75-85.

31. J. Rana and P. V. S. N. Murthy, Solute dispersion in pulsatile Casson fluid flow in a tube with wall absorption, *J. Fluid Mech.*, **793** (2016), 877-914.

32. A. K. Roy, A. K. Saha, and S. Debnath, On Dispersion in Oscillatory Annular Flow Driven Jointly by Pressure Pulsation and Wall Oscillation, *J. Appl. Fluid Mech.*, **10** (2017), 1487-1500.

33. A. K. Roy, A. K. Saha, and S. Debnath, Unsteady Convective Diffusion with Interphase Mass Transfer in Casson Liquid, *Period. Polytech. Chem. Eng.*, **62** (2018), 215-223.

34. R. Sankarasubramanian and W. N. Gill, Unsteady convective diffusion with interphase mass transfer, *Proc. R. Soc. London, Ser. A*, **333** (1973), 115-132.

35. A. Sarkar and G. Jayaraman, The effect of wall absorption on dispersion in annular flows, *Acta Mech.*, **158** (2002), 105-119.

36. A. Sarkar and G. Jayaraman, The effect of wall absorption on dispersion in oscillatory flow in an annulus: application to a catheterized artery, *Acta Mech.*, **172** (2004), 151-167.

37. G. I. Taylor, Dispersion of soluble matter in solvent flowing slowly through a tube, *Proc. R. Soc. London, Ser. A*, **219** (1953), 186-203.

38. Z. Wu and G. Q. Chen, Approach to transverse uniformity of concentration distribution of a solute in a solvent flowing along a straight pipe, *J. Fluid Mech.*, **740** (2014), 196-213.

39. Z. Wu, X. Fu, and G. Wang, Concentration distribution of contaminant transport in wetland flows, *J. Hydrol.*, **525** (2015), 335-344.

40. Z. Wu, X. Fu, and G. Wang, On spatial pattern of concentration distribution for Taylor dispersion process, *Sci. Rep.*, **6** (2016), 20556.

41. Z. Wu and A. Singh, On the effect of solute release position on plume dispersion, *J. Hydrol.*, **566** (2018), 607-615.

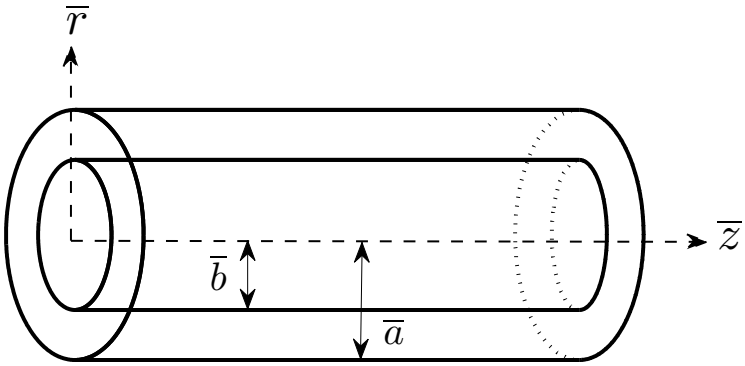

Fig. 1: Schematic diagram of the setup under consideration

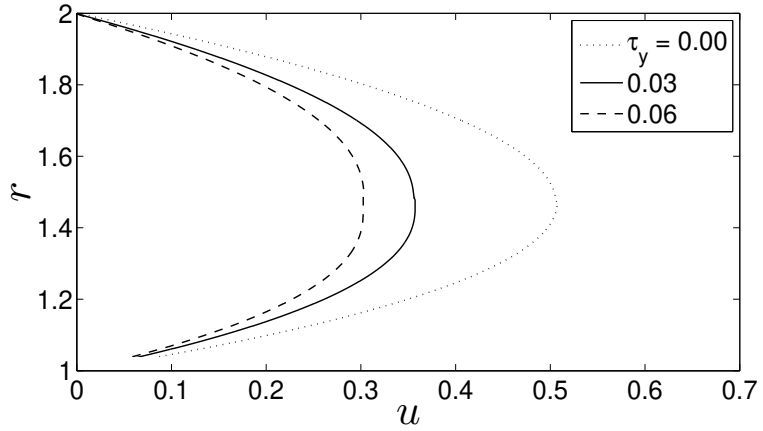

Fig. 2: The distribution of velocity for different values of yield stress τ_y.

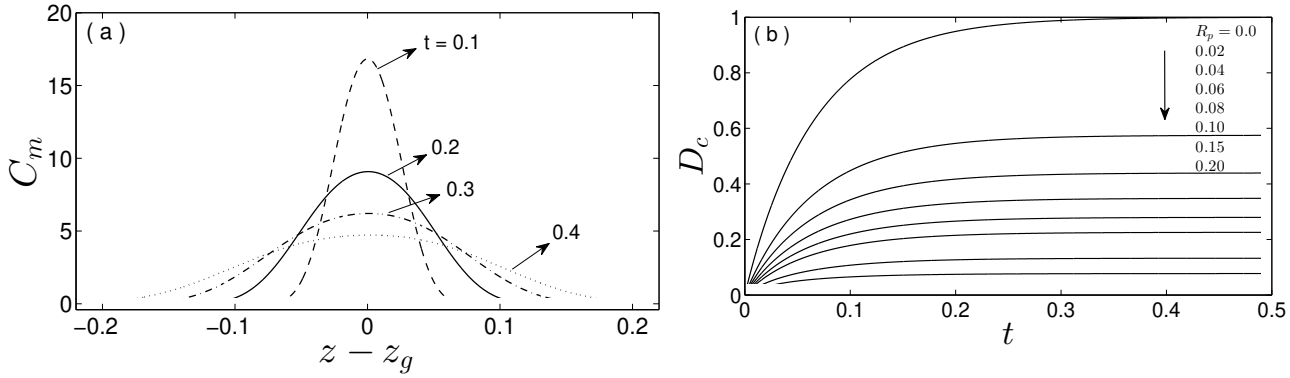

Fig. 3: (a) For combined flow (steady+unsteady), axial distribution of mean concentration at different times when $\eta \to 0$, $\tau_y = 0$, $\alpha = 1$, $e = 1.5$, and $\Gamma = 0$. (b) For steady flow, time variation of dispersion coefficient for different values of plug core radius when $\eta \to 0$, $e = 0$ and $\Gamma = 0$.

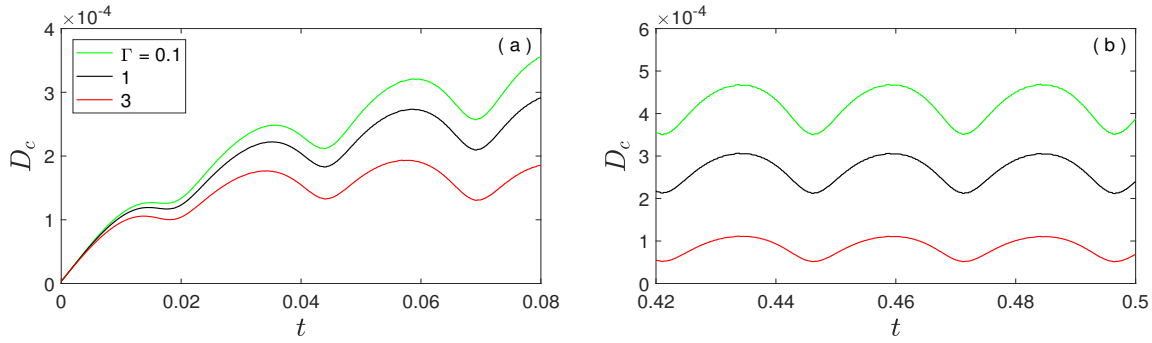

Fig. 4: Time variation of dispersion coefficient for different values of Γ when $\eta = 0.2$, $\tau_y = 0.04$, $\alpha = 0.5$, $e = 0.5$. (a) For small times; (b) for large times.

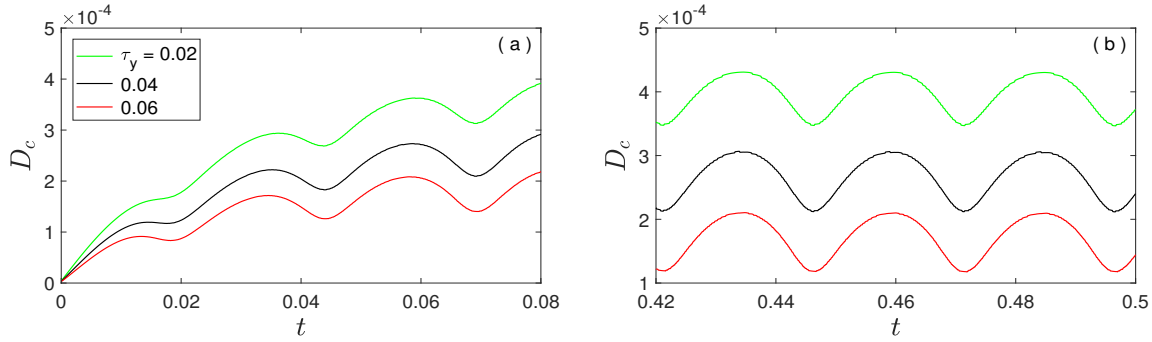

Fig. 5: Time variation of dispersion coefficient for different values of yield stress τ_y when $\eta = 0.2$, $\Gamma = 1$, $\alpha = 0.5$, $e = 0.5$. (a) For small times; (b) for large times.

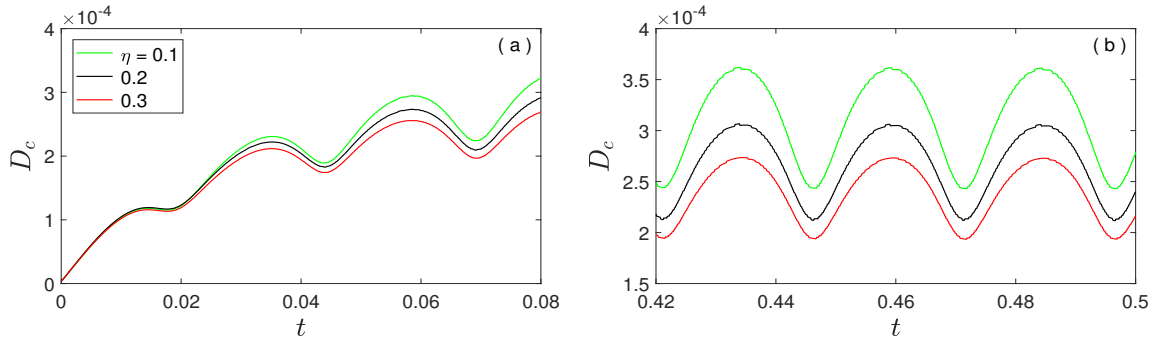

Fig. 6: Time variation of dispersion coefficient for different values of radius ratio η when $\tau_y = 0.04$, $\Gamma = 1$, $\alpha = 0.5$, $e = 0.5$. (a) For small times; (b) for large times.

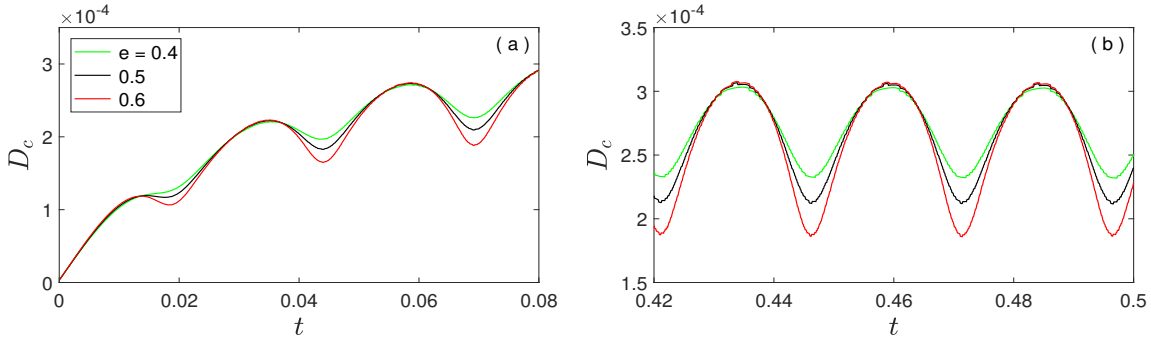

Fig. 7: Time variation of dispersion coefficient for different values of e when $\eta = 0.2$, $\tau_y = 0.04$, $\Gamma = 1$, $\alpha = 0.5$. (a) For small times; (b) for large times.

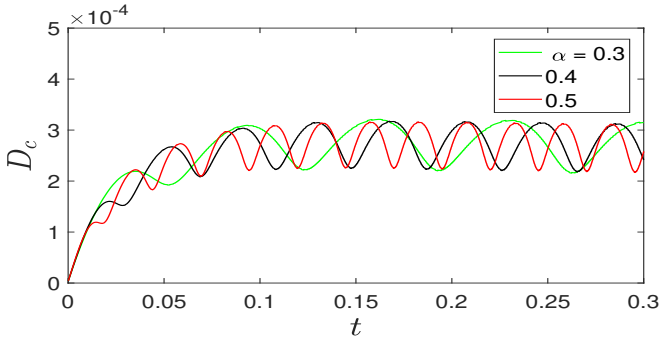

Fig. 8: Time variation of dispersion coefficient for different values of α when $\eta = 0.2$, $\tau_y = 0.04$, $\Gamma = 1$, $e = 0.5$. (a) For small times; (b) for large times.

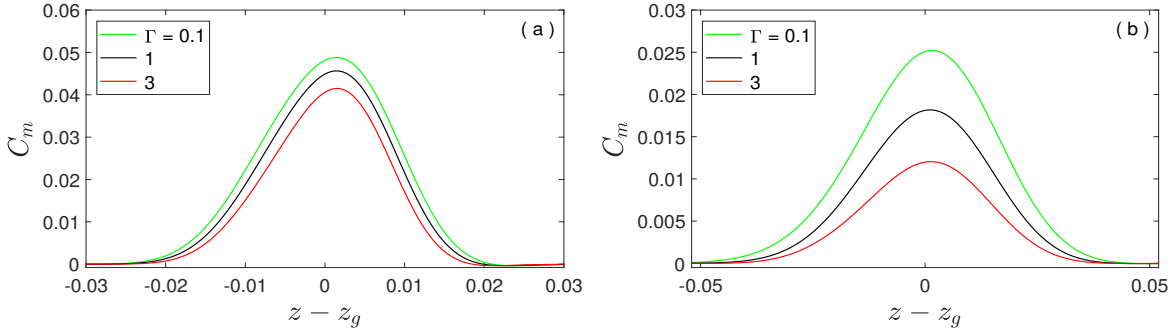

Fig. 9: Axial mean concentration distribution due to various Γ when $\eta = 0.2$, $\tau_y = 0.04$, $e = 0.5$, $\alpha = 0.5$. (a) At time $t = 0.15$; (b) at time $t = 0.5$.

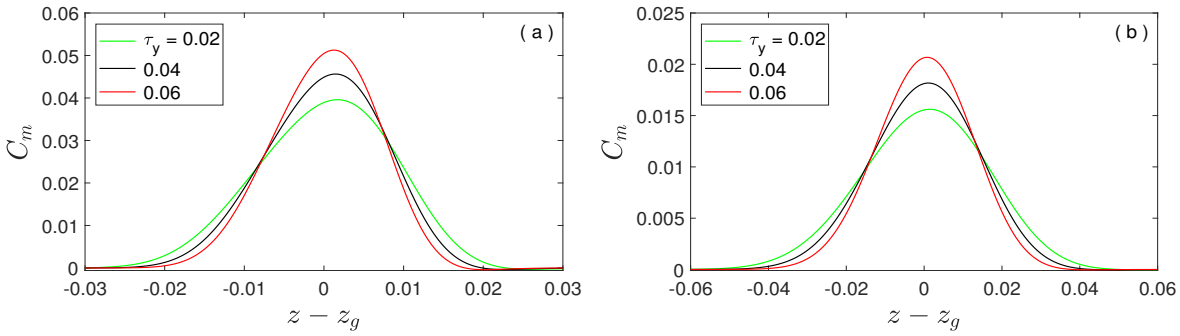

Fig. 10: Axial mean concentration distribution due to various τ_y when $\eta = 0.2$, $\Gamma = 1$, $\alpha = 0.5$, $e = 0.5$. (a) At time $t = 0.15$; (b) at time $t = 0.5$.

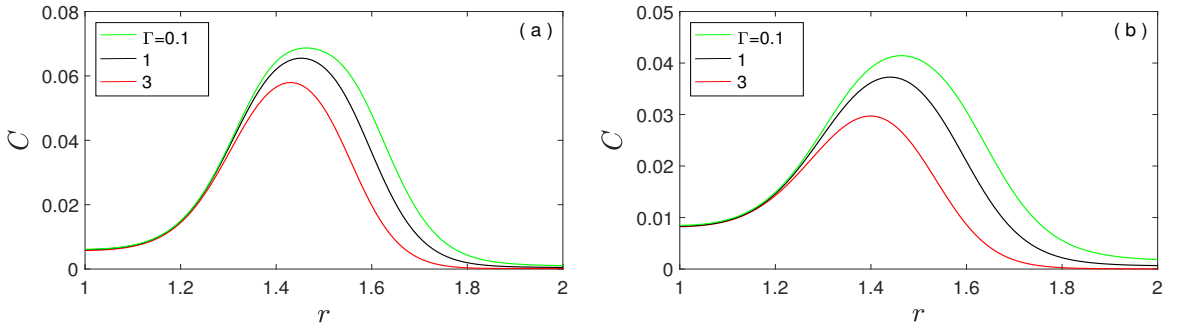

Fig. 11: Cross-sectional concentration distribution due to various Γ when $\eta = 0.5$, $\tau_y = 0.04$, $\alpha = 0.5$, $e = 0.5$, $z = 0.5$. (a) At time $t = 0.5$; (b) at time $t = 1$.

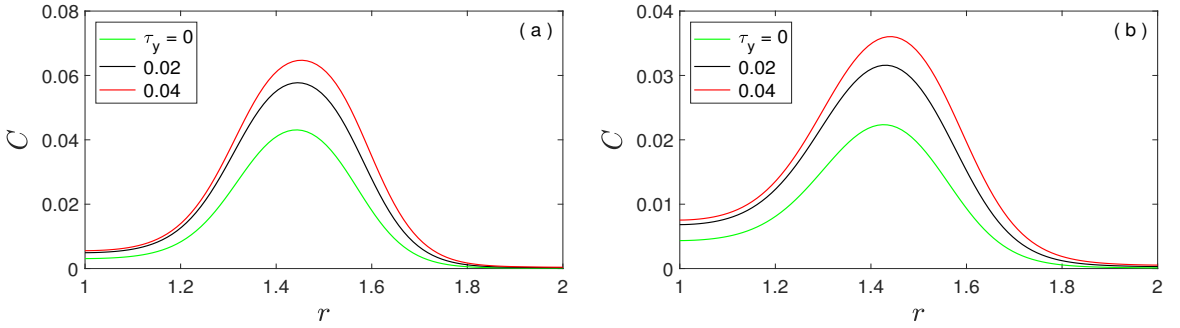

Fig. 12: Cross-sectional concentration distribution due to various τ_y when $\eta = 0.5$, $\Gamma = 1$, $\alpha = 0.5$, $e = 0.5$, $z = 0.5$. (a) At time $t = 0.5$; (b) at time $t = 1$.